Can extreme climatic events induce shifts in adaptive potential? A conceptual framework and empirical test with Anolis lizards

Monique Simon, Priscila Rothier, Colin Donihue, Anthony Herrel, Jason Kolbe

Can extreme climatic events induce shifts in adaptive potential? A conceptual framework and empirical test with *Anolis* lizards

Monique N. Simon

Department of Integrative Biology, Oklahoma State University, Stillwater OK, 74075, USA

monique.nouailhetas@gmail.com, orcid : 0000-0003-0106-2660

Priscila S. Rothier:

UMR 7179, Muséum National d'Histoire Naturelle, 75005 Paris, France,

priscilasrd@gmail.com, orcid: 0000-0003-3017-6528

Colin M. Donihue

Institute at Brown for Environment and Society, Brown University, Providence RI, 02912, USA, colindonihue@gmail.com, orcid : 0000-0003-1096-8536

Anthony Herrel

UMR 7179, Centre National de la Recherche Scientifique/ Muséum National d'Histoire Naturelle, 75005 Paris, France; Functional Morphology Lab, Department of Biology, University of Antwerp, B-2610 Wilrijk, Belgium; Evolutionary Morphology of Vertebrates, Ghent University, 9000 Ghent, Belgium, anthony.herrel@mnhn.fr

Jason J. Kolbe

Department of Biological Sciences, University of Rhode Island, Kingston RI, 02881, USA

jjkolbe@uri.edu

Abstract

Multivariate adaptation to climatic shifts may be limited by trait integration that causes genetic variation to be low in the direction of selection. However, strong episodes of selection induced by extreme climatic pressures may facilitate future population-wide responses if selection reduces trait integration and increases adaptive potential (i.e., evolvability). We

explain this counter-intuitive framework for extreme climatic events in which directional selection leads to increased evolvability and exemplify its use in a case study. We tested this hypothesis in two populations of the lizard *Anolis scriptus* that experienced hurricane-induced selection on limb traits. We surveyed populations immediately before and after the hurricane as well as the offspring of post-hurricane survivors, allowing us to estimate both selection and response to selection on key functional traits: forelimb length, hindlimb length, and toepad area. Direct selection was parallel in both islands and strong in several limb traits. Even though overall limb integration did not change after the hurricane, both populations showed a non-significant tendency toward increased evolvability after the hurricane despite the direction of selection not being aligned with the axis of most variance (i.e., body size). The population with comparably lower between-limb integration showed a less constrained response to selection. Hurricane-induced selection, not aligned with the pattern of high trait correlations, likely conflicts with selection occurring during normal ecological conditions that favors functional coordination between limb traits, and would likely need to be very strong and more persistent to elicit a greater change in trait integration and evolvability. Future tests of this hypothesis should use G-matrices in a variety of wild organisms experiencing selection due to extreme climatic events.

Introduction

Despite the vast literature focusing on adaptation to climate, predictions for how species will respond to climate change generally ignore the degree of adaptive potential of populations in the face of these changes, especially when multiple traits are under selection (Nadeau and Urban 2019; but see Etterson and Shaw 2001, Etterson 2004, Peschel et al. 2021). Adaptive responses to climatic pressures can alter ecological responses of populations, lowering their vulnerability to future changes, or even rescue populations from extinction (Quintero and

Wiens 2013, Diniz-Filho et al. 2019). Of course, these adaptive responses depend on standing genetic variation in the traits under selection, the frequency and severity of climatic perturbations that induce selection and even on interactions with other species (Grant et al. 2017). For instance, we may expect adaptation to be especially challenging in response to extreme climatic events that induce very strong episodes of selection, leading to high mortality and small population sizes that may never rebound. Given that extreme climatic events are likely to become more frequent and intense with future climate change, such as accelerating warming rate (Fischer et al. 2021), the potential of populations facing extreme events to adapt and persist may be limited. However, the scenario may not be so daunting if populations can increase their adaptive potential in response to predicted extreme climatic events.

In this paper, we lay out a conceptual framework for the intriguing possibility that directional selection may increase the adaptive potential of populations by reorganizing genetic variance such that it aligns more with the direction of selection (Pavlicev et al. 2011), such as when selection is caused by extreme climatic pressures. Then we show how to apply this framework with a case study of hurricane-induced selection on functional traits in *Anolis* lizards. Although our data set has some important limitations which we discuss, such as only phenotypic (and no genetic) data and limited sample sizes, our goal is to stimulate future research on evolvability and extreme climatic events, a theme that is currently underappreciated in the literature.

Genetic integration, constraint and evolvability

Given that selection induced by climate is likely on several traits at once, an important determinant of population-level responses is phenotypic and genetic integration among traits (Etterson and Shaw 2001). Theoretical models posit that if selection induced by changes in

76 the climate acts on several traits (i.e., multivariate selection; Lande 1979, Lande and Arnold
77 1983) that are tightly integrated—showing high genetic correlations—the response to
78 selection may deviate from the direction of selection (Hellmann and Pineda-Krch 2007,
79 Chevin 2012). Genetic trait integration is measured by the additive genetic variance-
80 covariance matrix, the G-matrix (*G*), which has trait variances along its diagonal and trait
81 covariances in the off-diagonal and characterizes the pattern of trait co-inheritance (Lande
82 1979, Arnold et al. 2008). The response to selection is then determined by an interaction
83 between directional selection and the G-matrix: $\Delta z = G\beta$; in which Δz is the evolutionary
84 response vector and β is the selection gradient, which measures only the direct selection on
85 traits by accounting for phenotypic trait correlations (Lande and Arnold 1983, Cheverud
86 1984).
87 High genetic integration among traits results in a very stretched G that accumulates
88 additive variance in only one or a few trait combinations (a 'cigar-shaped' G-matrix, in
89 contrast with a 'ball-shaped' G-matrix; see Figure 1), while most trait combinations will have
90 little additive genetic variance (Arnold et al. 2001, Walsh and Blows 2009). Therefore, the
91 shape of G (i.e., how genetic variance is distributed along trait combinations) is crucial for
92 determining how much additive variation will be available in the direction of β, that is, how
93 high is the evolvability or the ability of a population to adapt (Houle 1992, Hansen and Houle
94 2008). In highly integrated systems, if the direction of β is not aligned with the combinations
95 of traits accumulating genetic variance, *G* will have low evolvability in the direction of β and
96 Δz will deviate from the direction of selection (Arnold et al. 2001; scenario B in Figure 1).
97 Thus, whether populations will respond adaptively to climate-induced selection depends on
98 evolvability: the higher the evolvability, the more likely the response to selection will be
99 effectively adaptive. However, populations may be able to escape low evolvability if
100 selection induced by climate events can change the shape of G to become more aligned with

101 the direction of selection (i.e., more additive genetic variance in the direction of selection;
102 *e.g.*, Assis et al. 2016).
103
104 *Rapid shifts in evolvability and strong selection induced by climatic extremes*
105 Pavlicev et al. (2011) presented a theoretical model in which directional selection changes the
106 pattern of trait integration (i.e., changing the shape of *G*), by acting on genes that regulate the
107 degree of association between traits (the so-called 'rQTLs', relationship Quantitative Trait
108 Loci; Cheverud et al. 2004, Pavlicev et al. 2007). The fundamental idea is that rQTLs change
109 the effects of loci that control more than one trait (pleiotropic loci), which are one of the
110 genetic bases for trait correlations together with linkage disequilibrium. Therefore, this model
111 depends on genetic variation in pleiotropy, which was shown to be produced by interactions
112 of pleiotropic loci with different rQTLs (i.e., differential epistasis; Pavlicev et al. 2008).
113 Importantly, selection on rQTLs can change genetic variation without an appreciable effect
114 on trait means (Cheverud et al. 2004, Pavlicev et al. 2007). Thus, different genotypes at
115 rQTLs result in different G-matrices, and if they also show differences in mean fitness,
116 selection will favor a specific *G* and may culminate in changes in the population covariance
117 structure after several generations.
118 The most interesting result of this model is that *G* stretches in the direction of
119 selection, that is, the combination of traits with the highest additive variance gets aligned with
120 the direction of selection, increasing evolvability (Pavlicev et al. 2011). This happens because
121 the rQTL genotype with higher variance along the direction of selection has higher fitness.
122 The change in *G* is gradual across generations until the most advantageous genotype is fixed
123 by selection (Figure 2A). Hence, this model posits that directional selection can theoretically
124 change genetic trait integration to increase heritable variation in the direction of selection.
125 This is different from what is predicted with a more traditional view of selection acting

126 strictly on additive variation without epistasis, which would result in no change in genetic
127 variance, and therefore no change in evolvability after selection when considering
128 polygenetic traits and mutation-selection equilibrium (i.e., the genetic variation that is
129 removed by selection is replenished by mutation; Hill 1982, Burger 1993). However, both
130 the model of Pavlicev et al. (2011) and evolutionary simulations of the mutational matrix (M-
131 matrix; Jones et al. 2014, Melo and Marroig 2015) indicate that gene interactions (epistasis)
132 are a crucial factor to allow the alignment between the M-matrix, the G-matrix and
133 directional selection. More importantly, an increase in evolvability can happen quite fast,
134 only after 100 years of directional selection on chipmunks in natural conditions (Assis et al.
135 2016) and after 50 generations of artificial selection on mice (Penna et al. 2017).
136 If climate-induced selection elicits a change in *G* such that more additive variation
137 accumulates in the direction of selection, populations may be more prone to evolve
138 adaptively to the same climatic factor in the future, even if traits are strongly integrated
139 before the action of selection. This scenario may be even more relevant for population
140 survival in face of rapid climate change if selection induced by climatic events is strong.
141 Extreme climatic events, which are historically rare but increasing in frequency, may induce
142 strong episodes of directional selection (Grant et al. 2017). Such selection has the potential to
143 change not only trait means but also change the pattern of trait integration, culminating in a
144 shift in evolvability. It is important to note that the Pavlicev et al. (2011) simulations were
145 done with very weak selection (selection coefficients of 0.001 or 0.05), and still the change in
146 *G* could happen in less than 50 generations depending on the level of genetic linkage (Figure
147 2A, B). Yet, with very strong selection induced by extreme climatic pressures, a small change
148 in *G* could happen very fast, perhaps in just a single generation, but being enough to increase
149 evolvability in a biologically meaningful amount (Figure 2C).

We test this new hypothesis using lizard limb traits subjected to selection induced by hurricanes to demonstrate how this framework can be applied in future studies. Different from previous studies showing increased evolvability after selection (Pavlicev et al. 2008, Assis et al. 2016, Penna et al. 2017), we test this hypothesis on a system in which selection is not on the main axis of variation, which is body size here and in many other studies. It is unclear whether evolvability can increase with directional selection that is not aligned with the axis of greatest variation. In this case study, we use P-matrices as surrogates of G-matrices, and our results suggest that extreme climatic events could lead to increased evolvability in some populations. However, we caution that the ultimate test needs to be performed with G-matrices and larger sample sizes. An analytical framework developed by Grabowski and Porto (2017) can be used to estimate the minimum sample sizes needed to find significant changes in evolvability. Nevertheless, we emphasize that having ideal samples to study unpredictable extreme events in nature is quite difficult, and thus, we must work with the available data to reach an understanding of potential impacts of these increasingly common phenomena on biodiversity.

Case study: Hurricane-induced selection on lizard limb traits

We focused on two populations of the lizard *Anolis scriptus* that were exposed to Hurricanes Irma and Maria in 2017, showing strong selection on limb traits induced by this extreme climatic event (Donihue et al. 2018). In both populations, toepad area became larger, relative humerus length became longer, whereas relative femur length was shorter in survivors of the hurricane. These morphological changes were shown to be associated with higher clinging capacity and reduced aerodynamic drag, performances that are likely relevant to increase survival in the face of hurricanes (Donihue et al. 2018, Debaere et al. 2021). These populations were re-surveyed in 2019 and data on offspring of the survivors were

collected, allowing for the assessment of the degree to which the evolutionary responses to selection in the offspring (Δz) followed the direction of selection (β). Toepad area is likely heritable because the offspring of survivors from the hurricane also had large toepads (Donihue et al. 2020). Although this change could be due to phenotypic plasticity, limb traits are moderately to highly heritable. Narrow-sense heritability of hindlimb has been measured in *Anolis sagrei*, exhibiting quite high values (0.78 ± 0.13, see Calsbeek and Bonneaud 2008). Significant genetic variance on limb length was also measured in five species of *Anolis*, where heritabilities varied from 0.45 - 0.54 for femur and tibia, and around 0.15 for humerus and ulna (McGlothlin et al. 2018). Therefore, the limb structures of *Anolis* that we are dealing with comprise heritable traits that show additive variance that can be molded by selection.

Because we know that hurricane-induced selection is multivariate and limb traits are expected to be highly integrated in lizards, we need to analyze more than just a single trait for a robust understanding of the response to selection and whether evolvability changes after this episode of strong selection. Morphological integration of limb traits has been characterized in different *Anolis* species, showing that phenotypic correlations are generally high among limb elements (Kolbe et al. 2011). Recent studies in *Anolis* species revealed that genetic correlations are also high between limb traits (McGlothlin et al. 2018, 2021). High positive between-limb genetic correlations mean that it is easier to change all limb traits in the same direction (increasing or reducing all limb traits; directions that bear high genetic variation) than changing just fore- or hindlimb traits or changing fore- and hindlimb in different directions. We expect a similar pattern of high limb integration for *A. scriptus* populations (i.e., high positive correlations between fore- and hindlimbs), and that toepad area will be mostly correlated with the length of the corresponding longest finger or toe on which it was measured. Moreover, given that hurricane-induced selection resulted in an

increase in the lengths of forelimb traits, but a reduction in the lengths of hindlimb traits (Donihue et al. 2018), we expect the evolutionary response to selection in the offspring to have not followed the direction of selection because fore- and hindlimbs are genetically correlated in anoles (McGlothlin et al. 2018, 2021). Yet, we also expect to see an increase in evolvability in the offspring if hurricane-induced selection reduced correlations between the limbs (i.e., if selection reduced the overall integration of limb traits due to the opposing direction of selection on fore- and hindlimbs).

Methods

Sampling and morphological measurements

Anolis scriptus populations were sampled on two small islands in the Turks and Caicos: Pine Cay and Water Cay (350 and 250 ha, respectively). The islands are presently connected by a sandbar that was deposited by hurricane storm surge in the mid-1990s. However, the two populations are genetically distinct (unpublished data), and therefore can be treated as replicates of the response to extreme climatic events. Both cays are similarly covered by low vegetation (1 to 3 m in height). We sampled the anole populations along a 2-km transect on each island. The initial survey began on 28 August 2017 and lasted until 4 September 2017. We did not permanently mark individuals on the islands, and consequently, direct measures of individual survival are impossible. Hurricane Irma hit the Turks and Caicos on 8 September 2017 and Hurricane Maria passed through the region on 22 September 2017. Populations were revisited after the hurricanes between 16 October and 20 October 2017 and again approximately 18 months after the storms between 1 April 2019 and 8 April 2019. We caught 71 adult lizards in the initial survey, 93 during the 2017 revisit, and 117 lizards in 2019. This difference in sample size before and after the hurricane reflects an increased sampling effort after the hurricane. However, we do not expect these differences in sampling

to strongly affect selection differentials and response to selection because these metrics are calculated using sample means of surveyed populations, and means are generally well estimated with just a few individuals (although standard errors are generally higher with smaller sample sizes).

To identify the most likely offspring of hurricane survivors in 2019, we calculated the maximum body size of a lizard that had hatched on 1 April 2018, one year before our revisit (following Donihue et al. 2020). To do this, we used a logistic-by-length model and estimated growth rates in ecologically similar species to characterize the growth curve of lizards (see Donihue et al. 2020 for details). By excluding lizards larger than this size threshold, we conservatively estimated the subset of the sampled population less than a year old and thus, offspring of hurricane survivors. We retained for further analyses only the sexually mature adults of each sampling period (i.e., pre-hurricane / post-hurricane / offspring) by using an adult body size threshold for each sex. See Supplementary Material and Methods for a full description of the body size thresholds used. Our final sample sizes for each population were 36, 53 and 57 for Pine Cay, and 39, 52 and 57 for Water Cay, for pre-hurricane, post-hurricane, and offspring surveys, respectively.

All morphological measurements were taken by the same researcher on all three visits. Measurements included the snout-vent length (SVL), eight limb length segments, and toepad area on the fore- and hindlimbs (as described in Herrel et al. 2008; see also Lowie et al., 2019). For further details on the morphological measurements, see Supplementary Material.

Selection analysis and response to selection

To measure total hurricane-induced selection (indirect plus direct selection), we estimated a proxy of selection differentials (S), the mean trait difference between post- and

pre-hurricane sampling periods (S = [mean traits of post] – [mean traits of pre]), which represent the survivors after selection and the population before selection, respectively. The selection differential should be a difference between the mean of parents of the next generation, after the hurricane, and the mean of pre-hurricane populations, thus we are assuming that most survivors reproduced. We calculated separate selection differentials for each island, given that the populations are genetically distinct, and they differed in mean trait values in the pre-hurricane survey (Table S1). To measure only the direct selection on traits, we estimated the corresponding selection gradients (β) for each island. We used two different equations: $\beta = P^{-1}S$ and $\beta = P^{-1}\Delta z$ (Lande and Arnold 1983), where P^{-1} is the inverse of the phenotypic covariance matrix of limb traits in pre-hurricane populations and Δz is the response to selection. The second equation estimates β as the realized selection because it is based on the realized response to selection. We calculated the response to selection (Δz) for each island as the mean difference in traits between offspring and pre-hurricane populations. Inverting the P-matrix discounts the effects of trait correlations from the selection vector, retaining just direct selection on traits (Lande and Arnold 1983). However, given that P-matrices are estimated with sampling error, their inversion makes more error accumulate in the smallest eigenvalues (which dominate the inverted P-matrix), biasing estimates of selection gradients. To correct for this bias, we performed a sampling noise control approach following Marroig et al. (2012), in which we replace the smallest unreliable eigenvalues of P-matrices by the last reliable eigenvalue (which is the sixth one for the *A. scriptus* P-matrices, determined using the second derivative of the distribution of eigenvalues). This procedure has been shown to improve estimation of selection gradients (for more details, see Marroig et al. 2012). We explain below how we estimated P-matrices. Finally, we measured the vector correlation between both estimates of β to check if they are similar, and thus ensure that our assumption of post-hurricane population comprising mostly parents of the next generation

holds true. To determine the significance of vector correlations, we randomly sampled 1,000 vectors of 11 elements (number of traits) from a normal distribution of mean zero and unit SD and calculated their vector correlations. The critical values considering $\alpha = 0.05$ for this random distribution is -0.57 and 0.57. Therefore, any vector correlation below or above these values were considered significant.

To estimate uncertainty due to sampling error in our selection analysis, we performed bootstrapping of individuals caught on each survey in each island. We resampled with replacement 1,000 times for each population and then we calculated the selection metrics on resampled populations, resulting in 1,000 values of S and β. We extracted 95% confidence intervals (CI) for the selection metrics and if they did not encompass zero, the values were considered statistically significant. We also calculated 95% CI for mean-standardized selection to determine if hurricane-induced selection is strong compared to the literature (Hereford et al. 2004), and for Δz values to determine if the offspring showed significant changes.

P-matrices, overall integration and modularity of limb traits

We estimated P-matrices for each sampling period on each island to use as surrogates for G-matrices. Environmental effects leading to phenotypic plasticity may cause the P-matrix to differ from the G-matrix (Willis et al. 1991), but the potential for plasticity to impact traits in this study is likely low because growth after sexual maturity is limited. Moreover, Cheverud's conjecture has shown that well estimated G-matrices tend to resemble P-matrices (Cheverud 1988), especially for morphological traits with generally high heritabilities (i.e., high contribution of genetic factors to overall variance), which is the case for lizard limb traits. Moreover, empirical examples of similarity between G and P are mounting in the literature (e.g., Roff 1996, Phillips and Arnold 1999, Marroig and Cheverud 2001, Sodini et

al. 2019, Styga et al. 2019). Finally, we compared *A. scriptus* P-matrices with a G-matrix of the closest relative, *A. cristatellus*, extracted from McGlothlin et al. (2018), and matrices are substantially similar (see Supplementary Methods and Tables S2, S3). We also confirmed that P-matrices are reasonably well-estimated using a rarefaction analysis and we compared all P-matrices across populations of both islands (see Supplementary Methods and Figure S1). Given that $P = G + E$ (Falconer and Mackay, 1996), if P-matrices are similar, we may assume that P and G-matrices are also similar, otherwise the environmental matrix (E) in all populations would have to compensate for differences in G-matrices, which is a very unlikely scenario (Marroig and Cheverud 2001). Even though it is preferable to use estimates of G-matrices to test the hypothesis of increased evolvability with strong selection induced by climatic extremes, because the potential to adapt ultimately depends on heritable additive variation, estimating G-matrices in wild populations with appropriate sample sizes may be difficult. Despite this, the growing use of genomic data allowing the estimation of more precise G-matrices in a wide variety of organisms (Gienapp et al. 2017) will enable researchers to test this hypothesis more rigorously in the future.

To estimate mean overall integration of traits in both Pine and Water Cays, we used correlation P-matrices and calculated an integration index using the variance of eigenvalues (egv), which is less prone to bias due to differences in sample size compared to other integration metrics if negligible eigenvalues are excluded (O'Keefe et al. 2022). This index is a ratio between the variance of eigenvalues and its theoretical maximum, which simply corresponds to the number of traits minus one (Pavlicev et al. 2009). To test if egv values differed between surveys, we used the 1,000 bootstrapped populations to calculate 1,000 P-matrices for each survey and extract a 95% CI of overall integration for each survey. If the 95% CI did not overlap between-surveys, we considered the differences in egv significant. We performed this analysis for all traits (including SVL), and separately for forelimbs and

hindlimbs (excluding SVL) to check if one of the limbs showed a stronger response to hurricane-induced selection than the other.

We also performed a modularity analysis to explore the extent of integration of fore- and hindlimb components in relation to between-limb integration, and whether this pattern changed after the hurricanes. If the selection induced by the hurricane reduced the magnitude of between-limb correlations in the P-matrix, we expect to see an increase in limb modularity. We constructed three hypothetical modules: forelimb, hindlimb and toepad, the latter being composed of toepad area of fore- and hindlimbs as well as the longest finger and longest toe. Even though toepads are epidermal modifications that likely develop from an embryonic origin semi-independent from the skeletal limb elements (Weatherbee and Niswander, 2008; Liu et al., 2015; Gamble 2019), toepads are functionally linked to toes and fingers in locomotion (Ruibal and Ernst 1965; Elstrott and Irschick 2004), and therefore may constitute a functional module together with toes and fingers. We then tested whether average correlations within hypothetical modules (AVG+) were higher than between-modules (AVG-) using the empirical correlation P-matrices and a Mantel test to control for non-independence between correlations (Cheverud 1995, Porto et al. 2013; using function 'TestModularity' in evolqg R package, Melo et al. 2015). Although the Mantel test is effective in detecting biologically meaningful modules when the modularity hypotheses are grounded in well-established developmental and functional studies as is our case here, we also tested modularity using a more recent test, the Covariance Ratio coefficient (CR), and permutations to calculate significance of effect sizes using the R package *geomorph* (Adams and Otárola-Castillo 2013, Adams and Collyer 2019). The CR is based on a ratio of within- and between-module covariances and gives standardized effect sizes (using Z-score transformations that take the scale-dependence of traits into account) that characterize the strength of the modular signal (Adams and Collyer 2019).

Evolvability analysis

Evolvability measures the amount of genetic variation in *G* in the direction of selection ($e(\beta) = (\beta^T G\beta)/|\beta|^2$, where ^{T} means transpose and $|\beta|^2$ is the squared strength of selection; Hansen and Houle 2008). As we mentioned before, we substituted P-matrices for G-matrices to estimate evolvabilities. Thus, our interest was to compare evolvability in the directions of β before and after the hurricane to see if the P-matrices increased the amount of variation in the direction of selection, and to compare evolvability in the directions of β and Δz. If any of these vectors were aligned with trait correlations (i.e., aligned with pmax, the phenotypic equivalent of gmax), we expected their evolvability to be comparably high. To estimate the evolvability in the direction of selection, we then used the equation $e(\beta) = \beta^T P\beta$ (e.g., Assis et al. 2016; using function 'Evolvability' from evolqg R package, Melo et al., 2015) with β normalized to unit length and covariance P-matrices. Final $e(\beta)$ were standardized using the geometric mean of all traits to account for scale differences between traits and populations (e.g., Assis et al. 2016). We chose to standardize using a single value, the average geometric mean of traits, instead of using the mean of each trait (e.g., Hansen and Houle 2008) to preserve the structure of covariation.

We calculated two values of evolvability in the direction of selection for each island: (1) $e(\beta)$ before the hurricane: using pre-hurricane P-matrices and [post – pre] selection gradients, and (2) $e(\beta)$ after the hurricane: using offspring P-matrices and [post – pre] selection gradients. To estimate uncertainty in evolvability, we once again used the 1,000 bootstrapped values of β and the 1,000 bootstrapped P-matrices to construct 95% CI. This procedure accounts for error in estimation of both selection and P-matrices. We interpreted values as significantly different when 95% of the distributions did not overlap.

All analyses were conducted in the R programming environment (R Core Team 2021, version 4.1). We provide R scripts showing the selection and evolvability analyses, and showing the calculations to estimate inaccuracy in evolvability and number of individuals needed to achieve a certain level of accuracy in the Supplementary Materials.

Results

Hurricane-induced direct selection on limb traits and response to selection

Selection (*S*) was mostly negative on traits, however, we only found significant negative selection on the hindlimb longest toe in Pine Cay (Table 1). In contrast, we found that several selection gradients (β) were significant on both island populations—mostly negative in SVL and hindlimb traits and positive for toepads. We also found positive direct selection on the humerus, but it was only significant on Water Cay (Table 1). Results were similar when using β vectors estimated with either *S* or Δz, given that both ways of calculating β resulted in significantly similar vectors (i.e., vector correlations of 0.86 for Pine Cay and 0.93 for Water Cay, both above the critical value of 0.57). Moreover, selection was parallel in both islands, showing a vector correlation of 0.85. Interestingly, the mean-standardized β vectors are similar between-islands in magnitude, ranging from weak selection (around 0.05) to strong selection (around 0.7) when compared to the average mean-standardized β (0.89) found in Hereford et al. (2004) for morphological traits (see their Table 1). Response to selection (Δz) showed mostly a decrease in lengths of all traits, however, significant changes were only found in Pine Cay (Table 1). Δz vectors were not similar between populations, showing a non-significant vector correlation of 0.49. While the response to selection was aligned with β in Water Cay (vector correlation of 0.84), this was not the case for Pine Cay (vector correlation of 0.48), even though both β vectors are not correlated with the axis of highest phenotypic variance (vector correlations of 0.0 and 0.05, respectively). These results indicate that direct selection was

parallel across islands, not aligned with the direction of most phenotypic variance, and the response in the offspring differed between the two islands.

Pattern of limb trait correlations and overall integration

Correlation P-matrices are shown in Table S4. All correlation P-matrices show a PC1 that is predominantly isometric size, with similar magnitudes of loadings for all traits and all loadings with the same sign (Table S5). Also, PC1 explains high amounts of proportional variation in all surveys, showing that variance accumulates in the direction of size. However, the pre-hurricane population in Water Cay shows less proportional variation accumulated in PC1 compared with Pine Cay. All P-matrices show a very high similarity when using Random Skewers (RS), with all values above 0.91, indicating that matrices respond similarly to random selection. Similarity of the best matched PC axes (Krzanowski correlation, Krz) is in general lower, ranging from 0.70 to 0.79, which indicates that some PCs diverge across populations (Table 2). Still, P-matrices can be considered quite similar across populations, giving confidence in our assumption that *P* is a good surrogate of *G*.

We found a tendency for overall integration to be higher in post-hurricane populations, but the integration distributions overlap considerably (Figure 3A). The same pattern occurs if separating forelimb (95% CI for Pine Cay: pre = 0.21, 0.50; post = 0.36, 0.61; offspring = 0.19, 0.42; for Water Cay: pre = 0.12, 0.45; post = 0.25, 0.52; offspring = 0.18, 0.45; Figure 3B) and hindlimb (95% CI for Pine Cay: pre = 0.38, 0.73; post = 0.47, 0.73; offspring = 0.30, 0.60; for Water Cay: pre = 0.16, 0.5; post = 0.35, 0.65; offspring = 0.28, 0.60; Figure 3C). Results are the same if keeping all eigenvalues or just the first six eigenvalues. Therefore, mean limb trait integration did not change with the hurricane-induced selection.

Modularity of limb traits

The hindlimb is the only hypothetical module that shows higher average correlations within-module than between-modules, especially for Pine Cay populations (Figure 4). However, the hindlimb showed a signal of modularity that is significant only at P = 0.10 (Table S6). Therefore, forelimb, hindlimb and toepad traits can be seen as a single integrated unit. Still, we noticed that between-limb integration in pre-hurricane population was lower in Water Cay than in Pine Cay for both limbs (Figures 4B and 4C).

When using the CR coefficient, we found that both pre-hurricane populations have a significant CR coefficient. However, CR values are above 1.0 indicating that covariances within-modules are lower than between-modules. Moreover, we found no differences in pairwise comparisons of CR effect sizes across populations (Table S7, Figure S2). Therefore, we confirmed our results from the Mantel test that the limbs are a single integrated unit in all populations and that the pattern did not change after the hurricane.

Evolvability

We found a similar trend of increased evolvability in the direction of β from pre-hurricane parents to offspring in both islands (Table 3). However, the simulated confidence intervals are quite large, making these differences non-significant. This lack of significance may be due to low sample size to detect an evolvability difference. To determine the level of accuracy in our evolvability values, we used the analytical framework developed by Grabowski and Porto (2017), in which we could calculate the inaccuracy of evolvability given our sample size (lowest in pre-hurricane populations, around 35 individuals) and the overall integration of P-matrices (from 0.5 to 0.6). By looking at Figure S3A, our inaccuracy in evolvability ranged from 0.05 to 0.06. We also determined how many individuals we would need to find a significant difference (accuracy of 0.03 or lower) given the overall integration of P-matrices: we would need at least 65 to 75 individuals (Figure S3B).

Table 1. Selection differentials (*S*), selection gradients (β), and response to selection (Δz) separated by island. We show empirical values and the bootstrapped 95% CI. CI in bold are significant.

Selection and Response to Selection							
Pine Cay	**Traits**	**S (post -pre)**	**95% CI**	**β (post - pre)**	**95% CI**	**Δz (off - pre)**	**95% CI**
Total size	SVL	-0.028	-0.088, 0.036	-0.187	**-0.269, -0.099**	-0.060	-0.124, 0.005
Hindlimb	femur	-0.068	-0.133, 0.002	-0.179	**-0.253, -0.099**	-0.081	**-0.149, -0.010**
	tibia	-0.033	-0.095, 0.034	-0.080	-0.160, 0.002	-0.054	-0.119, 0.0112
	metatarsal	-0.033	-0.089, 0.028	0.003	-0.062, 0.071	-0.062	**-0.123, -0.002**
	longest toe	-0.073	**-0.134, -0.008**	-0.303	**-0.413, -0.200**	-0.074	**-0.140, -0.008**
	toepad area	0.057	-0.110, 0.230	0.186	**0.103, 0.265**	-0.068	-0.237, 0.100
Forelimb	humerus	-0.017	-0.085, 0.057	0.062	-0.030, 0.161	-0.021	-0.087, 0.048
	radius	-0.034	-0.093, 0.032	-0.095	**-0.160, -0.030**	-0.065	**-0.125, -0.007**
	metacarp	-0.024	-0.080, 0.036	-0.048	-0.102, 0.008	0.012	-0.049, 0.071
	longest finger	-0.040	-0.101, 0.030	-0.021	-0.085, 0.044	-0.040	-0.113, 0.031
	toepad area	0.083	-0.075, 0.216	0.094	**0.035, 0.150**	-0.026	-0.195, 0.143
Water Cay	**Traits**	**S (post -pre)**	**95% CI**	**β (post - pre)**	**95% CI**	**Δz (off - pre)**	**95% CI**
Total size	SVL	-0.010	-0.065, 0.047	-0.101	**-0.146, -0.053**	-0.028	-0.085, 0.030
Hindlimb	femur	-0.067	-0.137, 0.004	-0.290	**-0.394, -0.187**	-0.064	-0.130, 0.006
	tibia	-0.009	-0.068, 0.051	-0.051	-0.129, 0.025	-0.024	-0.087, 0.037
	metatarsal	0.000	-0.055, 0.059	-0.014	-0.067, 0.042	-0.035	-0.094, 0.022
	longest toe	-0.030	-0.089, 0.033	-0.172	**-0.247, -0.101**	-0.023	-0.085, 0.040
	toepad area	0.086	-0.074, 0.248	0.069	**0.010, 0.129**	0.046	-0.120, 0.218
Forelimb	humerus	0.034	-0.028, 0.100	0.132	**0.067, 0.200**	0.009	-0.057, 0.075,
	radius	-0.005	-0.061, 0.054	-0.045	-0.090, 0.005	-0.026	-0.087, 0.034
	metacarp	0.031	-0.025, 0.093	-0.004	-0.065, 0.060	-0.003	-0.067, 0.062
	longest finger	0.021	-0.050, 0.091	0.023	-0.055, 0.099	-0.011	-0.079, 0.058
	toepad area	0.098	-0.061, 0.256	0.119	**0.050, 0.182**	0.038	-0.123, 0.205

Table 2. Matrix similarity between all P-matrices. We used two methods to compare P-matrices. Random Skewers (RS) indicates the similarity in the response to random selection, whereas Krzanowski correlation (Krz) indicates similarity based on the best matched pairs of eigenvectors. All values are significant at $\alpha = 0.05$.

Matrix similarity		
Pine Cay	RS	Krz
pre x post	0.96	0.76
pre x offspring	0.95	0.73
post x offspring	0.94	0.74
Water Cay	RS	Krz
pre x post	0.92	0.71
pre x offspring	0.92	0.79
post x offspring	0.96	0.75
Pine Cay x Water Cay	RS	Krz
pre	0.91	0.7
post	0.97	0.74
offspring	0.94	0.79

Table 3. Empirical evolvabilities and associated 95% confidence intervals.

Evolvabilities	**pre e(β)**	**offspring e(β)**
Pine Cay	0.15	0.20
95% CI (simulations)	0.11, 0.19	0.14, 0.25
Water Cay	0.11	0.19
95% CI (simulations)	0.08, 0.22	0.14, 0.39

Discussion

Incorporating multivariate adaptive responses of populations to climate change is a necessary step to better predict how and which species may overcome these challenges (Peschel et al. 2020). However, if climate-induced selection acts on multiple traits simultaneously and if traits are highly integrated, the response to selection may be constrained, not closely following the direction of selection (Etterson and Shaw 2001, Hellmann and Pineda-Krch 2007, Chevin 2012). In this scenario, populations may not be able to cope with climate change even when responding to selection because the response would lead to a lower increase in mean fitness given that some traits will respond non-adaptively. This is especially likely if genetic correlations between positively selected traits are negative (e.g., Etterson and Shaw 2001), but also if selection is not aligned with axes accumulating the most variance in the G-matrix (Arnold et al. 2001, Blows and Walsh 2009). Yet, if selection also changes the pattern of trait integration and increases the amount of genetic variance aligned with selection, future response to this same selection may be facilitated (Pavlicev et al. 2011). These alternative scenarios ultimately depend on the extent to which trait integration results in only a few directions accumulating most of the genetic variance, and how much selection is aligned with these directions (showing high evolvability; scenario B in Figure 1) or whether selection changes trait integration to increase evolvability.

We investigated these possibilities in a case study of an extreme climatic event, hurricane-induced selection on lizard limb traits (Donihue et al. 2018, 2020), in which we had samples of survivors and their offspring for two different populations. Given that selection was inferred to be strong on some of the limb traits (Donihue et al. 2018), we hypothesized that selection would change the pattern of limb integration and re-distribute genetic variation in a way that would increase the chance of adaptation to hurricanes in the future. Because we could not estimate G-matrices for the populations, our results are only suggestive, but

indicate that both populations had higher evolvability in the direction of selection after the hurricane, although this result was not significant. This lack of significance may be more related to a low sample size than to a genuinely non-significant effect, as we calculated that a sample size of around 70 individuals with the same evolvability values would lead to enough accuracy to find significant difference in evolvability before and after the hurricane. Interestingly, our results raise the possibility that evolvability may increase after a single episode of selection and even if the direction of selection is not aligned with size (or PC1, the direction accumulating most genetic variance). Still, using P-matrices as surrogates of G-matrices likely may have overestimated evolvability values if environmental variation contributes to total variation in the direction of selection. Alternatively, environmental variation may be much higher along pmax than gmax given that this direction is related to size, and several environmental factors can affect growth. In this case, evolvabilities can be underestimated by using P-matrices instead of G-matrices.

The model of directional selection influencing evolvability predicts changes in the pattern of correlation even with fluctuating selection, but the change depends on the level of epistasis between rQTLs and other genes (Pavlicev et al. 2011). Hence, it may be that only sustained or frequent directional selection, such as maintaining the same direction for several generations, would be able to increase evolvability in the direction of selection. Although we do not expect hurricane-induced selection to be this persistent because of its infrequency, lizard populations experiencing periodic hurricanes (up to four hurricanes over a 70-year period) show larger toepads than populations exposed to fewer hurricanes (Donihue et al. 2020), indicating that hurricanes can leave persistent marks on phenotypes. Moreover, hurricane frequency and magnitude are predicted to increase in the future due to climate change (Bender et al. 2010, Knutson et al. 2010).

Direction of selection, locomotor performance and variation in responses to selection

Direct selection on limb traits in Pine Cay and Water Cay populations was parallel, giving some confidence in their estimation with the sampling noise control approach when inverting P-matrices (Marroig et al. 2012). Parallel selection was also found in other lizard systems inferred to have suffered hurricane-induced selection (e.g., Rabe et al. 2020). Direct selection was strong in several limb traits, but not so strong on toepad area, although selection gradients were towards increased surface area, and this is likely related to increased clinging capacity in *A. scriptus* (Crandell et al. 2014, Donihue et al. 2018). However, shifts in toepad area do not always lead to higher clinging capacity in lizards (e.g., Dufour et al. 2019) and other traits beyond toepad area also change clinging capacity (such as setae length and limb length; Hagey et al. 2014, Kolbe 2015). Direct selection to reduce femur length was stronger, supporting the evidence in favor of reduced aerodynamic drag in lizards that have smaller hindlimbs and consequently exposing less of the pelvic region to the strong winds induced by hurricanes (Debaere et al. 2021). Thus, selection induced by hurricanes, and possibly selection induced by other climatic events, may vary in direction and strength on different traits, showing the relevance of using a multivariate approach to estimate selection.

Another source of variation induced by climatic events is how much the responses are constrained by trait integration. Fore- and hindlimbs compose a single integrated unit in both populations. This high between-limb integration was expected from previous studies (Kolbe et al. 2011, McGlothlin et al. 2018) and likely results from the need to coordinate both limbs in locomotion (Aerts et al. 2000). However, populations may still differ in the strength of between-limb integration. For instance, the modularity analysis showed that between-limb correlations were lower in Water Cay than in Pine Cay, and the former had a morphological response that followed much more closely the direction of selection than Pine Cay (vector correlation of 0.84 compared with 0.48, respectively). Because direct selection was not

aligned with limb integration in either of the populations (i.e., selection did not increase or decrease all limb traits, as evidenced by the lower correlation between β and pmax), the lower correlations between limbs may have resulted in less correlated responses of limb elements in Water Cay, and therefore, a lower constraint in the direction of the response to selection. Finally, we must also consider that populations may differ due to chance and evolutionary forces unrelated to selection and having more than two populations in future studies will aid in evaluating the consistency of patterns of selection and responses to selection induced by hurricanes.

Therefore, although extreme climatic events like hurricanes are predicted to become more frequent and intense with future climate change (Bender et al. 2010, Knutson et al. 2010), the responses of lizard populations may vary because of differences in strength of selection, and differences in trait integration resulting in different degrees of constrained responses to selection. A broader implication of all these sources of variation for responses to climate-driven selective pressures is the resultant variation in how long these changes last in terms of evolutionary time. For traits experiencing stronger selection and having lower genetic correlations, a longer-lasting evolutionary response to extreme climatic events may be more common, as shown for populations and species more often hit by hurricanes showing larger toepads (Donihue et al. 2020). On the other hand, for traits that show a more constrained response because of high trait integration, the evolutionary responses may be more ephemeral.

Selection on trait integration patterns and evolvability

Even though we found evidence for strong selection on some limb traits in both populations, integration patterns were not changed by this selection, suggesting that only very strong selection (or lesser magnitude of selection sustained over multiple generations) can

583 redistribute variation in the G-matrix. For instance, in two different species of chipmunks that
584 experienced selection induced by 100 years of climate change, only the species under
585 stronger selection showed increased evolvability after selection (Assis et al. 2016). Whether
586 strong selection changes trait integration, and perhaps also evolvability, may be related to a
587 conflict with multivariate stabilizing selection (Cheverud 1984, Roff and Fairbain 2012)
588 associated with maintenance of a pattern of higher correlations among traits that perform the
589 same function. In this scenario, the G-matrix is kept evolutionary conserved by a stable
590 pattern of correlational selection, that in the case of lizard limbs would be associated with
591 locomotor tasks normally performed in the environment (e.g., sprinting, jumping, climbing;
592 Irschick and Losos 1998, Perry et al. 2004, Foster and Higham 2012). These performances
593 demand a coordination between fore- and hindlimbs, and thus selection to enhance these
594 performances would favor high integration between limbs (McGlothlin et al. 2018). This
595 conflict between episodes of directional selection causing short-term, fast changes in *G*, and
596 multivariate stabilizing selection promoting long-term evolutionary stability in *G*, must be
597 common in nature given that different types of selection may act on populations (Arnold et
598 al., 2008). Selective forces and other factors, such as mutation, all influence simultaneously
599 the G-matrix and the balance between these factors ultimately shape the evolutionary
600 potential of populations. Therefore, hurricane-induced selection on *A. scriptus* limbs in the
601 Turks and Caicos appears to conflict with selection associated with normal environmental
602 conditions with the latter being much more persistent. Hence, the P- and G-matrices of *A.*
603 *scriptus* are likely shaped by multivariate selection related to normal limb functioning to a
604 much greater extent than by hurricane-induced selection, even if these extreme selection
605 events are much stronger than selection in normal ecological conditions. Even for populations
606 subjected to hurricanes in a higher frequency, selection in normal ecological conditions may

erase any potential long-lasting signal of lower limb integration due to hurricane-induced selection.

Conclusion

We showed how the hypothesis of directional selection leading to increased evolvability can be studied in the context of population-wide responses to extreme climatic events. Ideally, this hypothesis should be tested with G-matrices with appropriate sample sizes before and after the extreme event, which are likely above 70 individuals if studying around 10 traits. Although we expected strong hurricane-induced selection to reduce limb trait integration, this did not happen in *A. scriptus* populations, potentially because the episodic selection caused by this hurricane was not persistent enough to contrast normal ecological conditions, despite hurricanes being a relatively strong selective force. Even so, our results indicate that evolutionary responses follow more closely the direction of selection if between-limb integration is lower. Therefore, persistence of populations facing strong environmental changes may be enhanced by lower trait integration, even if individuals perform normal functions at a lower level than more highly integrated individuals in normal ecological conditions.

References

Adams, D.C. and Otárola-Castillo, E. (2013). geomorph: an R package for the collection and analysis of geometric morphometric shape data. Methods in Ecology and Evolution 4, 393-399.

Adams, D.C. and Collyer, M.L. (2019). Comparing the strength of modular signal, and evaluating alternative modular hypotheses, using covariance ratio effect sizes with morphometric data. Evolution 73, 2352-2367.

632 Aerts, P., Van Damme, R., Vanhooydonck, B., Zaaf, A., & Herrel, A. (2000). Lizard
633 locomotion: how morphology meets ecology. Netherlands Journal of Zoology 50, 261-278.

634 Andrews, R.B. (1982). Patterns of growth in reptiles. In Biology of the Reptilia, (Academic
635 Press), pp. 273–320.

636 Arnold, S.J., Pfrender, M.E., and Jones, A.G. (2001). The adaptive landscape as a conceptual
637 bridge between micro- and macroevolution. In Microevolution Rate, Pattern, Process, A.P.
638 Hendry, and M.T. Kinnison, eds. (Dordrecht: Springer Netherlands), pp. 9–32.

639 Arnold, S.J., Bürger, R., Hohenlohe, P.A., Ajie, B.C., and Jones, A.G. (2008). Understanding
640 the evolution and stability of the G-matrix. Evolution 62, 2451–2461.

641 Assis, A.P.A., Patton, J.L., Hubbe, A., and Marroig, G. (2016). Directional selection effects
642 on patterns of phenotypic (co)variation in wild populations. Proceedings of the Royal Society
643 B: Biological Sciences 283, 20161615.

644 Bender, M.A., Knutson, T.R., Tuleya, R.E., Sirutis, J.J., Vecchi, G.A., Garner, S.T., and
645 Held, I.M. (2010). Modeled Impact of Anthropogenic Warming on the Frequency of Intense
646 Atlantic Hurricanes. Science 327, 454-458.

647 Blows, M.W., Chenoweth, S.F., and Hine, E. (2004). Orientation of the Genetic Variance-
648 Covariance Matrix and the Fitness Surface for Multiple Male Sexually Selected Traits. The
649 American Naturalist 163, 329–340.

650 Burger, R. (1993). Prediction of the dynamics of a polygenic character under directional
651 selection. Journal of Theoretical Biology 162, 487-513.

652 Calsbeek, R. and Bonneaud, C. (2008). Postcopulatory fertilization bias as a form of cryptic
653 sexual selection. Evolution, 62, 1137-1148.

654 Cheverud, J.M. (1984). Quantitative genetics and developmental constraints on evolution by
655 selection. Journal of Theoretical Biology 110, 155–171.

656 Cheverud, J.M. (1988). A comparison of genetic and phenotypic correlations. Evolution 42,
657 958-968.

Cheverud, J.M. (1995). Morphological Integration in the Saddle-Back Tamarin (Saguinus fuscicollis) Cranium. The American Naturalist 145, 63–89.

Cheverud, J.M., and Marroig, G. (2007). Research Article Comparing covariance matrices: random skewers method compared to the common principal components model. Genet. Mol. Biol. 30, 461–469.

Cheverud, J.M., Ehrich, T.H., Vaughn, T.T., Koreishi, S.F., Linsey, R.B., and Pletscher, L.S. (2004). Pleiotropic effects on mandibular morphology II: Differential epistasis and genetic variation in morphological integration. J. Exp. Zool. 302B, 424–435.

Chevin, L.-M. (2012). Genetic constraints on adaptation to a changing environment. Evolution 67, 708–721.

Crandell, K.E., Herrel, A., Sasa, M., Losos, J.B., and Autumn, K. (2014). Stick or grip? Co-evolution of adhesive toepads and claws in Anolis lizards. Zoology 117, 363–369.

Debaere, S.F., Donihue, C.M., Herrel, A., and Van Wassenbergh, S. (2021). An aerodynamic perspective on hurricane-induced selection on Anolis lizards. Functional Ecology n/a.

Diniz-Filho, J.A.F., Souza, K.S., Bini, L.M., Loyola, R., Dobrovolski, R., Rodrigues, J.F.M., Lima-Ribeiro Matheus de, S., Terribile, L.C., Rangel, T.F., Bione, I., et al. (2019). A macroecological approach to evolutionary rescue and adaptation to climate change. Ecography 42, 1124–1141.

Donihue, C.M., Herrel, A., Fabre, A.-C., Kamath, A., Geneva, A.J., Schoener, T.W., Kolbe, J.J., and Losos, J.B. (2018). Hurricane-induced selection on the morphology of an island lizard. Nature 560, 88–91.

Donihue, C.M., Kowaleski, A.M., Losos, J.B., Algar, A.C., Baeckens, S., Buchkowski, R.W., Fabre, A.-C., Frank, H.K., Geneva, A.J., Reynolds, R.G., et al. (2020). Hurricane effects on Neotropical lizards span geographic and phylogenetic scales. Proc Natl Acad Sci USA 117, 10429–10434.

Dufour, C.M.S., Donihue, C.M., Losos, J.B., and Herrel, A. (2019). Parallel increases in grip strength in two species of Anolis lizards after a major hurricane on Dominica. J Zool 309, 77–83.

686 Elstrott, J., and Irschick, D.J. (2004). Evolutionary correlations among morphology, habitat
687 use and clinging performance in Caribbean Anolis lizards. Biological Journal of the Linnean
688 Society 83, 389–398.

689 Etterson, J.R. (2004). Evolutionary potential of Chamaecrista fasciculata in relation to
690 climate change. II. Genetic architecture of three populations reciprocally planted along an
691 environmental gradient in the Great Palins. Evolution 58, 1459–1471.

692 Etterson, J.R., and Shaw, R.G. (2001). Constraint to Adaptive Evolution in Response to
693 Global Warming. Science 294, 151-154.

694 Falconer, D.S. and Mackay, T. (1996). Introduction to Quantitative Genetics. 4th Edition,
695 Addison Wesley Longman, Harlow.

696 Fischer, E.M., Sippel, S., and Knutti, R. (2021). Increasing probability of record-shattering
697 climate extremes. Nature Climate Change, 11, 689-695.

698 Foster, K.L., and Higham, T.E. (2012). How forelimb and hindlimb function changes with
699 incline and perch diameter in the green anole, Anolis carolinensis. Journal of Experimental
700 Biology 215, 2288–2300.

701 Gamble, T. (2019). Duplications in Corneous Beta Protein Genes and the Evolution of Gecko
702 Adhesion. Integrative and Comparative Biology 59, 193–202.

703 Gienapp, P., Fior, S., Guillaume, F., Lasky, J.R., Sork, V.L., and Csilléry, K. (2017).
704 Genomic quantitative genetics to study evolution in the wild. Trends in Ecology &
705 Evolution 32, 897-908.

706 Goswami, A., and Finarelli, J.A. (2016). EMMLi: A maximum likelihood approach to the
707 analysis of modularity. Evolution 70, 1622–1637.

708 Grant, P.R., Grant, B.R., Huey, R.B., Johnson, M.T.J., Knoll, A.H., and Schmitt, J. (2017).
709 Evolution caused by extreme events. Philosophical Transactions of the Royal Society B:
710 Biological Sciences 372, 20160146.

711 Grabowski, M., and Porto, A. (2017). How many more? Sample size determination in studies
712 of morphological integration and evolvability. Methods in ecology and evolution, 8, 592-603.

713 Hagey, T.J., Puthoff, J.B., Holbrook, M., Harmon, L.J., and Autumn, K. (2014). Variation in
714 setal micromechanics and performance of two gecko species. Zoomorphology 133, 111–126.

715 Hansen, T.F., and Houle, D. (2008). Measuring and comparing evolvability and constraint in
716 multivariate characters. Journal of Evolutionary Biology 21, 1201–1219.

717 Hellmann, J.J., and Pineda-Krch, M. (2007). Constraints and reinforcement on adaptation
718 under climate change: Selection of genetically correlated traits. Biological Conservation 137,
719 599–609.

720 Hereford, J., Hansen, T.F., and Houle, D. (2004). Comparing strengths of directional
721 selection: how strong is strong? Evolution 58, 2133-2143.

722 Herrel, A., Damme, R.V., Vanhooydonck, B., Zaaf, A., and Aerts, P. (2000). Lizard
723 Locomotion: How Morphology Meets Ecology. Netherlands Journal of Zoology 50, 261–
724 277.

725 Herrel, A., Huyghe, K., Vanhooydonck, B., Backeljau, T., Breugelmans, K., Grbac, I., Van
726 Damme, R., and Irschick, D.J. (2008). Rapid large-scale evolutionary divergence in
727 morphology and performance associated with exploitation of a different dietary resource.
728 Proceedings of the National Academy of Sciences 105, 4792–4795.

729 Hill, W.G. (1982). Rates of change in quantitative traits from fixation of new mutations.
730 Proceedings of the National Academy of Sciences USA 79, 142-145.

731 Houle, D. (1992). Comparing evolvability and variability of quantitative traits. Genetics 130,
732 195–204.

733 Irschick, D.J., and Losos, J.B. (1998). A comparative analysis of the ecological significance
734 of maximal locomotor performance in Caribbean Anolis lizards. Evolution 52, 219–226.

735 Jones, A.G., Bürger, R., and Arnold, S.J. (2014). Epistasis and natural selection shape the
736 mutational architecture of complex traits. Nat Commun 5, 3709.

737 Knutson, T.R., McBride, J.L., Chan, J., Emanuel, K., Holland, G., Landsea, C., Held, I.,
738 Kossin, J.P., Srivastava, A.K., and Sugi, M. (2010). Tropical cyclones and climate change.
739 Nature Geoscience 3, 157–163.

740 Kolbe, J.J. (2015). Effects of Hind-Limb Length and Perch Diameter on Clinging
741 Performance in Anolis Lizards from the British Virgin Islands. Journal of Herpetology 49,
742 284–290.

743 Kolbe, J.J., Revell, L.J., Szekely, B., Brodie III, E.D., and Losos, J.B. (2011). Convergent
744 evolution of phenotypic integration and its alignment with morphological diversification in
745 Caribbean Anolis ecomoprhs. Evolution 65, 3608–3624.

746 Krzanowski, W.J. (1979). Between-GroupCsomparison of Principal. Journalof the American
747 Statistical Association 5, 703-707.

748 Lande, R. (1979). Quantitative Genetic Analysis of Multivariate Evolution, Applied to Brain:
749 Body Size Allometry. Evolution 33, 402-416.

750 Lande, R. and Arnold, S.J. (1983). The measurement of selection on correlated characters.
751 Evolution 37, 1210-1236.

752 Liu, Y., Zhou, Q., Wang, Y., Luo, L., Yang, J., Yang, L., Liu, M., Li, Y., Qian, T., Zheng, Y.,
753 et al. (2015). Gekko japonicus genome reveals evolution of adhesive toe pads and tail
754 regeneration. Nature Communications 6, 10033.

755 Lowie, A., Gillet, E., Vanhooydonck, B., Irschick, D.J., Losos, J.B., and Herrel, A. (2019).
756 Do the relationships between hind limb anatomy and sprint speed variation differ between
757 sexes in Anolis lizards? Journal of Experimental Biology jeb.188805.

758 Marroig, G., and Cheverud, J.M. (2001). A comparison of phenotypic variation and
759 covariation patterns and the role of phylogeny, ecology, and ontogeny during cranial
760 evolution of New World monkeys. Evolution 55, 2576-2600.

761 Marroig, G., Melo, D. A., and Garcia, G. (2012). Modularity, noise, and natural
762 selection. Evolution 66, 1506-1524.

763 McGlothlin, J.W., Kobiela, M.E., Wright, H.V., Mahler, D.L., Kolbe, J.J., Losos, J.B., and
764 Brodie, E.D. (2018). Adaptive radiation along a deeply conserved genetic line of least
765 resistance in Anolis lizards. Evolution Letters 2, 310–322.

766 McGlothlin, J.W., Kobiela, M.E., Wright, H.V., and Kolbe, J.J. (2021) The Adaptive
767 Radiation of Anolis lizards. bioRxiv, 46.

768 Melo, D., and Marroig, G. (2015). Directional selection can drive the evolution of modularity
769 in complex traits. Proceedings of the National Academy of Sciences 112, 470-475.

770 Melo, D., Garcia, G., Hubbe, A., Assis, A.P., and Marroig, G. (2015). EvolQG: An R
771 package for evolutionary quantitative genetics. F1000Research 4: 925.

772 Nadeau, C.P., and Urban, M.C. (2019). Eco-evolution on the edge during climate change.
773 Ecography 42, 1280–1297.

774 O'Keefe, F.R., Meachen, J.A., and Polly P.D. (2022). On Information Rank Deficiency in
775 Phenotypic Covariance Matrices. Systematic Biology, 71, 810-822.
776
777 Pavlicev, M., Kenney-Hunt, J.P., Norgard, E.A., Roseman, C.C., Wolf, J.B., and Cheverud,
778 J.M. (2007). Genetic variation in pleiotropy: Differential epistasis as a source of variation in
779 the allometric relationship between long bone lengths and body weight. Evolution 62, 199-
780 213.

781 Pavlicev, M., Kenney-Hunt, .JP., Norgard, E.A., Roseman, C.C., Wolf, J.B., and Cheverud,
782 J.M. (2008). Genetic variation in pleiotropy: Differential epistasis as a source of variation in
783 the allometric relationship between long bone lengths and body weight. Evolution, 62, 199–
784 213.
785
786 Pavlicev, M., Cheverud, J. M., and Wagner, G. P. (2009). Measuring morphological
787 integration using eigenvalue variance. Evolutionary Biology, 36, 157-170.

788 Pavlicev, M., Cheverud, J.M., and Wagner, G.P. (2011). Evolution of adaptive phenotypic
789 variation patterns by direct selection for evolvability. Proceedings of the Royal Society B:
790 Biological Sciences 278, 1903–1912.

791 Pearson, P.R., and Warner, D.A. (2018). Early hatching enhances survival despite beneficial
792 phenotypic effects of late-season developmental environments. Proceedings of the Royal
793 Society B: Biological Sciences 285, 20180256.

794 Penna, A., Melo, D., Bernardi, S., Oyarzabal, M I., & Marroig, G. (2017). The evolution of
795 phenotypic integration: How directional selection reshapes covariation in mice. Evolution 71,
796 2370-2380.

797 Perry, G., LeVering, K., Girard, I., and Garland, T. (2004). Locomotor performance and
798 social dominance in male Anolis cristatellus. Animal Behaviour 67, 37–47.

799 Peschel, A.R., Boehm, E.L., and Shaw, R.G. (2021). Estimating the capacity of Chamaecrista
800 fasciculata for adaptation to change in precipitation. Evolution 75, 73–85.

801 Phillips, P.C., and Arnold, S.J. (1999). Hierarchical Comparison of Genetic Variance-
802 Covariance Matrices. I. Using the Flury Hierarchy. Evolution 53, 1506-1515.

803 Porto, A., Shirai, L.T., de Oliveira, F.B., and Marroig, G. (2013). Size variation, growth
804 strategies, and the evolution of modularity in the Mammalian skull. Evolution 67, 3305–
805 3322.

806 Quintero, I., and Wiens, J.J. (2013). What determines the climatic niche width of species?
807 The role of spatial and temporal climatic variation in three vertebrate clades. Global Ecology
808 and Biogeography 22, 422–432.

809 Rabe, A.M., Herrmann, N.C., Culbertson, K.A., Donihue, C.M., and Prado-Irwin, S.R.
810 (2020). Post-hurricane shifts in the morphology of island lizards. Biological Journal of the
811 Linnean Society 130, 156–165.

812 Revell, L.J., Mahler, D.L., Sweeney, J.R., Sobotka, M. Fancher, V.E. and Losos, J.B. (2010).
813 Nonlinear selection and the evolution of variances and covariances for continuous characters
814 in an anole. Journal of Evolutionary Biology 23, 407–421.

815 Roff, D.A. (1996). The evolution of genetic correlations: An analysis of patterns. Evolution
816 50, 1392–1403.

817 Roff, D.A., and Fairbairn, D.J. (2012). A test of the hypothesis that correlational selection
818 generates genetic correlations. Evolution 66, 2953–2960.

819 Rothier, P.S., Brandt, R., and Kohlsdorf, T. (2017). Ecological associations of autopodial
820 osteology in Neotropical geckos. Journal of Morphology 278, 290–299.

821 Ruibal, R., and Ernst, V. (1965). The structure of the digital setae of lizards. Journal of
822 Morphology 117, 271–293.

Sodini, S.M., Kemper, K.E., Wray, N.R., and Trzaskowski, M. (2019). Comparison of Genotypic and Phenotypic Correlations: Cheverud's Conjecture in Humans, Genetics 209, 941–948.

Styga, J.M., Houslay, T.M., Wilson, A.J., and Earley, R.L. (2019). Development of G: a test in an amphibious fish. Heredity 122, 696–708.

Walsh, B., and Blows, M.W. (2009). Abundant Genetic Variation + Strong Selection = Multivariate Genetic Constraints: A Geometric View of Adaptation. Annu. Rev. Ecol. Evol. Syst. 40, 41–59.

Weatherbee, S.D., and Niswander, L.A. (2008). Chapter 7. Mechanisms of Chondrogenesis and Osteogenesis in Limbs. B.K. Hall, ed. (University of Chicago Press), pp. 93–102.

Willis, J.H., Coyne, J.A., and Kirkpatrick, M. (1991). Can One Predict the Evolution of Quantitative Characters Without Genetics? Evolution 45, 441–444.

Wright, A.N., Piovia-Scott, J., Spiller, D.A., Takimoto, G., Yang, L.H., and Schoener, T.W. (2013). Pulses of marine subsidies amplify reproductive potential of lizards by increasing individual growth rate. Oikos 122, 1496–1504.

Figure legends

Figure 1. Visual representation of the G-matrix and its interaction with directional selection (β) to produce an evolutionary response (Δz). The G-matrix is generally represented by the directions of its first and second axes of variation (PC1 or pmax, and PC2, respectively). Selection is represented as a selection surface (or fitness landscape, blue contour lines) and the direction of selection (blue arrows). In scenario **A**, the G-matrix has low integration between traits, showing a *ball-shaped representation*. Because the genetic integration is low, the evolutionary response (red arrows) follows the direction of selection independent of the position of populations in relation to the selection surface. In scenario **B**, the G-matrix has high integration between traits, showing a *cigar-shaped representation*, with

most variance accumulating in the direction of gmax. In this scenario, the evolutionary response may not follow the direction of selection, representing a case of genetic constraint, as shown for population 1 (Pop 1). However, if selection is aligned with gmax (Pop 2) or with PC2 (Pop 3), the evolutionary response will follow the direction of selection even with high genetic integration between traits. Figure adapted from Arnold et al. 2001.

Figure 2. Conceptual framework of directional selection shifting evolvability. A) A population under strong sustained selection gradually changes its G-matrix (elipse) to first become less integrated and then aligning completely with the direction of selection, leading to increased evolvability. Adapted from Assis et al. (2016). **B)** Under weak sustained selection, we expect the G-matrix to show lower integration only after some generations (50 generations in this example). **C)** Under very strong selection, such as the one induced by extreme climatic events, the G-matrix may show lower integration in just a single generation, also increasing evolvability in the direction of selection, despite not being completely aligned with the direction of selection.

Figure 3. Mean overall integration of limb traits and toepad area. The values are eigenvalue variance of correlation P-matrices. **A)** All traits. **B)** Forelimb traits. **C)** Hindlimb traits. The distributions were constructed by bootstrap resampling with 1,000 iterations.

Figure 4. Average correlations within (w) and between (b) the three hypothetical modules. A) Pine Cay. **B)** Water Cay. Boxplots are showing the average correlation as a horizontal line. A set of traits is considered a module when within-set average correlation is higher than between-set average correlation. See table S2 for the results of the modularity tests.

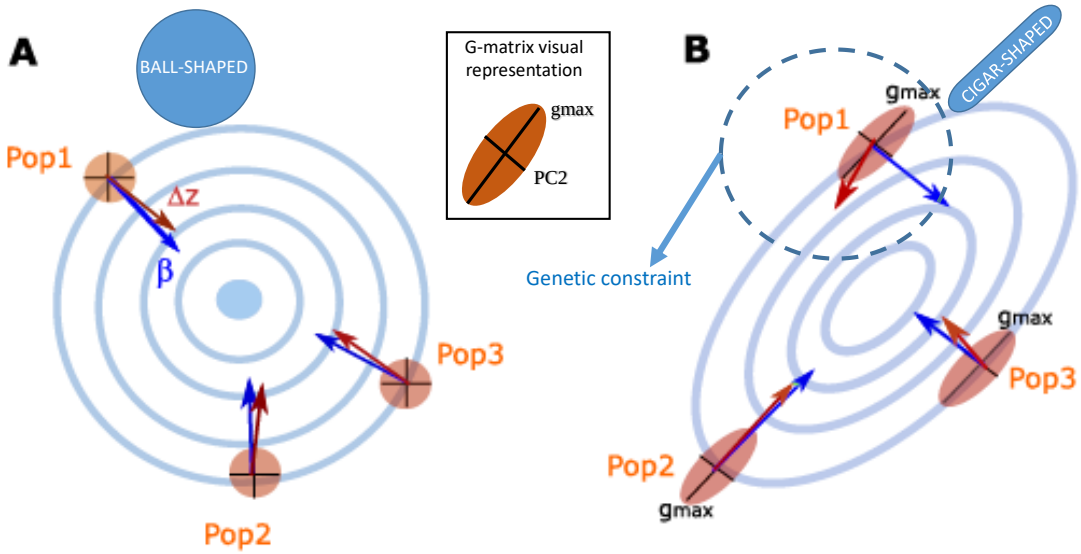
A
BALL-SHAPED
Pop1
Δz
β
Pop3
Pop2
G-matrix visual representation
gmax
PC2
B
CIGAR-SHAPED
gmax
Pop1
Genetic constraint
gmax
Pop3
Pop2
gmax

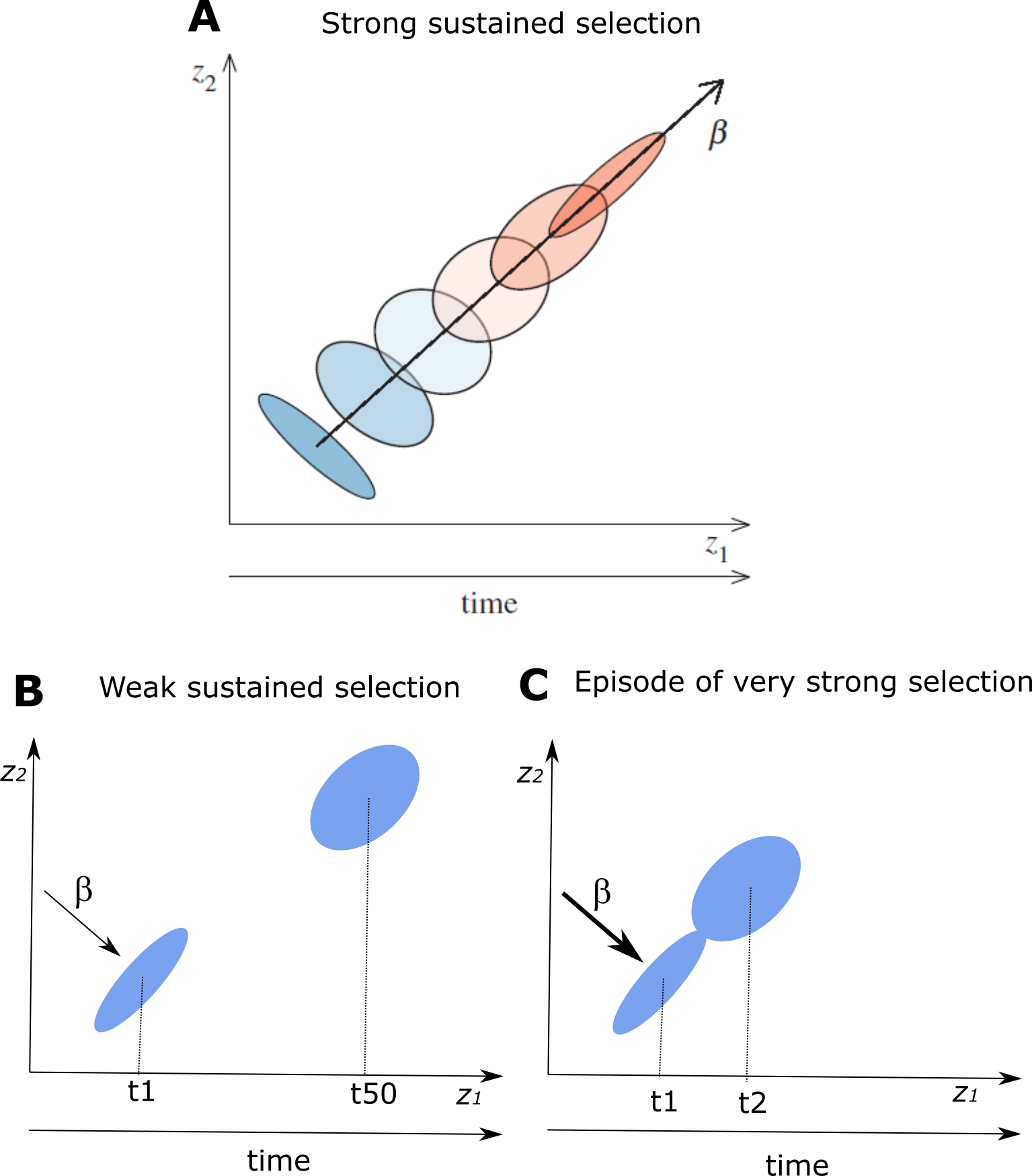
A
Strong sustained selection
z_2
β
z_1
time
B
Weak sustained selection
z_2
β
t1
t50
z_1
time
C
Episode of very strong selection
z_2
β
t1
t2
z_1
time

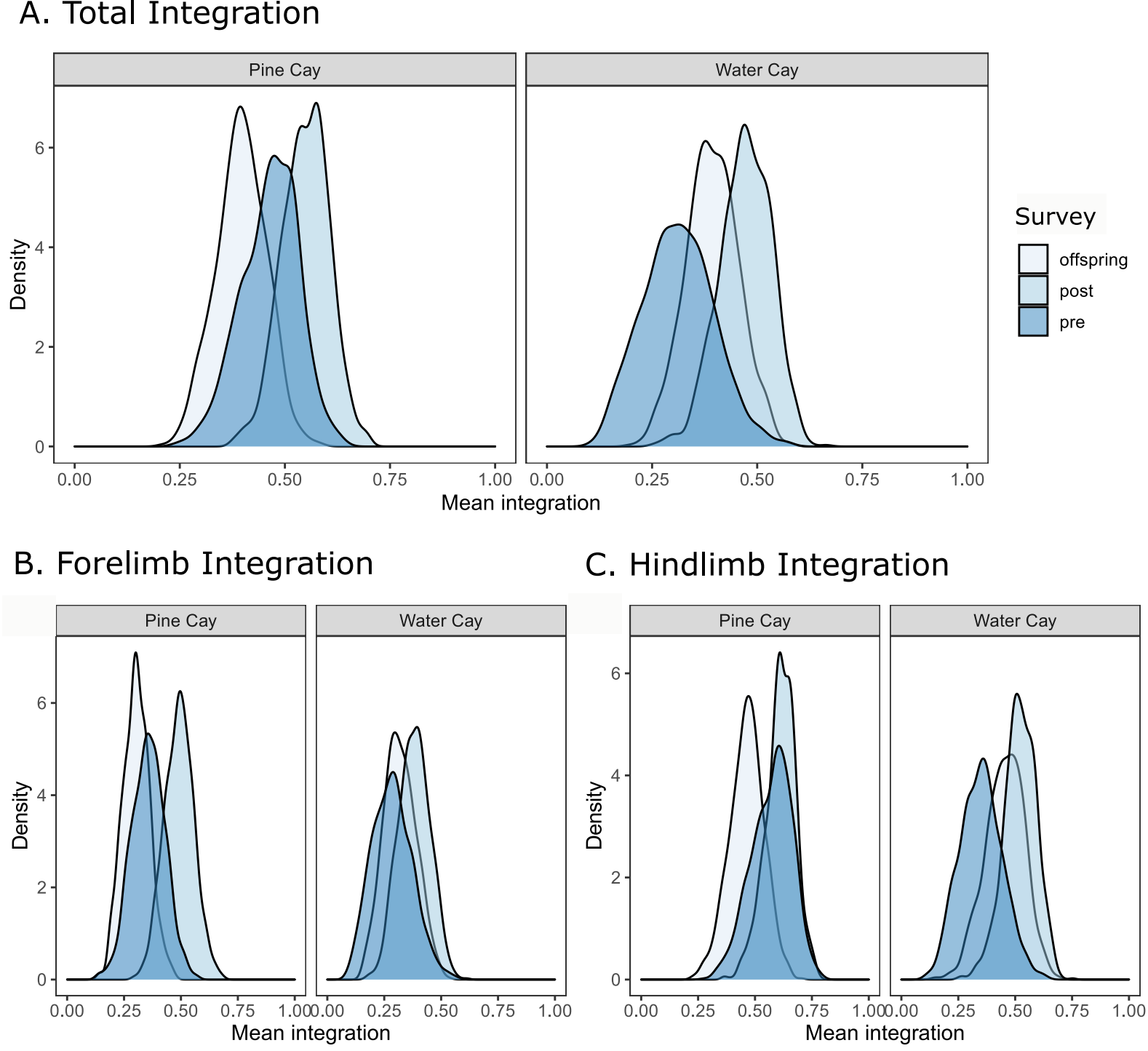
A. Total Integration
Pine Cay
Water Cay
Density
Mean integration
Survey
offspring
post
pre
B. Forelimb Integration
C. Hindlimb Integration

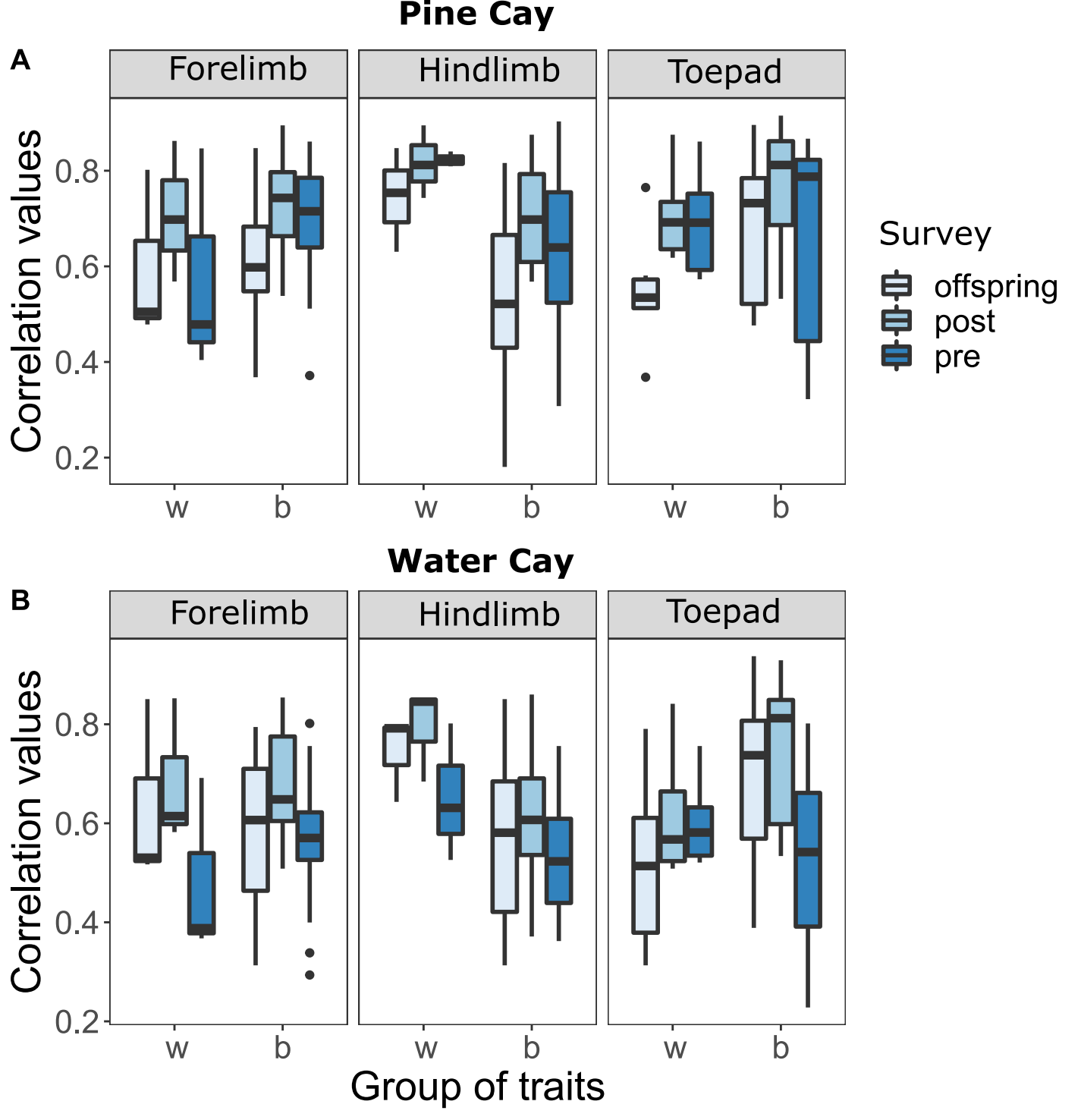
Pine Cay
A
Forelimb
Hindlimb
Toepad
Correlation values
0.8
0.6
0.4
0.2
w
b
Survey
offspring
post
pre
Water Cay
B
Group of traits